

2

## Dicke Narrowing in Strong Fields: The Atom-as-Antenna Analogy

Prepared by

J. C. CAMPARO and R. P. FRUEHOLZ  
Electronics Technology Center  
Technology Operations

and

H. G. ROBINSON  
Physics Department, Duke University  
Durham, NC 27706

13 May 1992

Prepared for

SPACE SYSTEMS DIVISION  
AIR FORCE SYSTEMS COMMAND  
Los Angeles Air Force Base  
P. O. Box 92960  
Los Angeles, CA 90009-2960

DTIC  
ELECTE  
JUL 01 1992  
S B D

Contract No. F04701-88-C-0089

Engineering and Technology Group

THE AEROSPACE CORPORATION  
El Segundo, California

92 6 22 112

92-17120

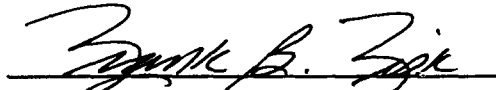
This report was submitted by The Aerospace Corporation, El Segundo, CA 90245-4691, under Contract No. F04701-88-C-0089 with the Space Systems Division, P. O. Box 92960, Los Angeles, CA 90009-2960. It was reviewed and approved for The Aerospace Corporation by B. K. Janousek, Principal Director, Electronics Technology Center. Mr. Franklin Fisk was the project officer for the Mission-Oriented Investigation and Experimentation (MOIE) program.

This report has been reviewed by the Public Affairs Office (PAS) and is releasable to the National Technical Information Service (NTIS). At NTIS, it will be available to the general public, including foreign nationals.

This technical report has been reviewed and is approved for publication. Publication of this report does not constitute Air Force approval of the report's findings or conclusions. It is published only for the exchange and stimulation of ideas.



MARTIN K. WILLIAMS, Capt, USAF  
Mgr, Space Systems Integration  
DCS for Program Management



FRANKLIN B. FISK, GM-14, DAF  
Deputy Chief, Space Sensors Division

UNCLASSIFIED

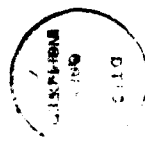
SECURITY CLASSIFICATION OF THIS PAGE

## REPORT DOCUMENTATION PAGE

1a. REPORT SECURITY CLASSIFICATION Unclassified			1b. RESTRICTIVE MARKINGS	
2a. SECURITY CLASSIFICATION AUTHORITY			3. DISTRIBUTION/AVAILABILITY OF REPORT  Approved for public release; distribution unlimited.	
2b. DECLASSIFICATION/DOWNGRADING SCHEDULE				
4. PERFORMING ORGANIZATION REPORT NUMBER(S)  TR-0089(4945-05)-1			5. MONITORING ORGANIZATION REPORT NUMBER(S)  SSD-TR-92-10	
6a. NAME OF PERFORMING ORGANIZATION The Aerospace Corporation Technology Operations		6b. OFFICE SYMBOL (if applicable)	7a. NAME OF MONITORING ORGANIZATION  Space Systems Division	
6c. ADDRESS (City, State, and ZIP Code)  El Segundo, CA 90245			7b. ADDRESS (City, State, and ZIP Code) Los Angeles Air Force Base Los Angeles, CA 90009-2960	
8a. NAME OF FUNDING/SPONSORING ORGANIZATION		8b. OFFICE SYMBOL (if applicable)	9. PROCUREMENT INSTRUMENT IDENTIFICATION NUMBER  F04701-88-C-0089	
8c. ADDRESS (City, State, and ZIP Code)			10. SOURCE OF FUNDING NUMBERS	
			PROGRAM ELEMENT NO.	PROJECT NO.
			TASK NO.	WORK UNIT ACCESSION NO.
11. TITLE (Include Security Classification)  Dicke Narrowing in Strong Fields: The Atom-as-Antenna Analogy				
12. PERSONAL AUTHOR(S) Camparo, James C. and Frueholz, Robert P. (The Aerospace Corporation) and Robinson, H. G. (Duke University)				
13a. TYPE OF REPORT		13b. TIME COVERED FROM _____ TO _____	14. DATE OF REPORT (Year, Month, Day) 1992 May 13	15. PAGE COUNT 20
16. SUPPLEMENTARY NOTATION				
17. COSATI CODES			18. SUBJECT TERMS (Continue on reverse if necessary and identify by block number)  Atomic clocks Dicke narrowing	
FIELD	GROUP	SUB-GROUP		
19. ABSTRACT (Continue on reverse if necessary and identify by block number) When a radiator (or absorber) suffers velocity-changing collisions that do not perturb its internal state, the oscillator's successive Doppler shifts are motionally averaged. This process (Dicke narrowing) gives rise to a homogeneously broadened sub-Doppler resonance, which is often astride a broad, apparently Doppler width, pedestal. It has long been held that this pedestal is an inhomogeneous remnant of Doppler broadening, but no evidence has ever been obtained to substantiate this expectation. In the present study we investigate the behavior of Dicke-narrowed lineshapes in strong fields in an evacuated wall-coated cell. Our experimental results indicate that the hypothesis of an inhomogeneous Doppler remnant pedestal is invalid. Rather, the pedestal is homogeneously broadened, and is best understood in terms of the oscillator's response to the electromagnetic field's power spectral density as observed in its rest frame. This conclusion suggests an intimate relationship between the process of Dicke narrowing and the behavior of quantum systems in the presence of stochastic fields. By envisioning the quantum system as a narrow-band antenna that only absorbs a small portion of the field's energy, we develop a simple intuitive model to account for the interaction of the atom with the nonmonochromatic field; the appeal of this simple theory is that it removes the need for extensive computation. Agreement between this "atom-as-antenna" analogy and experiment is very good.				
20. DISTRIBUTION/AVAILABILITY OF ABSTRACT <input checked="" type="checkbox"/> UNCLASSIFIED/UNLIMITED <input type="checkbox"/> SAME AS RPT. <input type="checkbox"/> DTIC USERS			21. ABSTRACT SECURITY CLASSIFICATION  Unclassified	
22a. NAME OF RESPONSIBLE INDIVIDUAL			22b. TELEPHONE (Include Area Code)	22c. OFFICE SYMBOL

## Preface

We wish to thank Spencer Delcamp for his help in performing the experiments.



Accession For	
NTIS GRA&I	<input checked="checked" type="checkbox"/>
DTIC TAB	<input type="checkbox"/>
Unannounced	<input type="checkbox"/>
Justification	
By _____	
Distribution/	
Availability Codes	
Dist	Avail and/or Special
A-1	

## CONTENTS

PREFACE .....	1
I. INTRODUCTION .....	5
II. EXPERIMENT .....	9
III. RESULTS AND ANALYSIS .....	11
A. Saturation Broadening .....	11
B. Empirical Model of the Atom-as-Antenna .....	13
C. Light Narrowing of Dicke Pedestals .....	16
IV. SUMMARY AND CONCLUSION .....	19
REFERENCES .....	21

## FIGURES

1. Typical Dicke-narrowed lineshape as obtained in our experiment: a narrow central-resonance spike sitting on top of a broad pedestal .....	5
2. (a) Optical-pumping, double-resonance experimental arrangement for observing the $\text{Rb}^{87}$ 0-0 hyperfine transition lineshape, and (b) energy level diagram of $\text{Rb}^{87}$ showing atomic transitions of interest .....	9
3. Saturation behavior of full signal amplitude, spike signal amplitude, and the pedestal amplitude .....	11
4. Power broadening behavior of the pedestal. ....	12
5. Predicted lineshapes in the atom-as-antenna analogy .....	15
6. Saturation broadening of the pedestal linewidth in the atom-as-antenna analogy .....	16
7. Observation of anomalous pedestal narrowing .....	17

## I. INTRODUCTION

Roughly thirty years ago Dicke (Refs. 1,2) considered the problem of a quantum mechanical oscillator emitting (or absorbing) radiation of wavelength  $\lambda$  in a static, one-dimensional potential well of spatial extent  $\alpha$ . He recognized that if  $\alpha$  was less than or equal to  $\lambda$ , then the radiation spectrum of the oscillator would consist of a sub-Doppler central resonance (spike) sitting on top of a broad pedestal as illustrated in Figure 1. For his simple illustrative situation, Dicke found that the width of the narrow central resonance was equal to the radiator's natural dephasing rate, while the broad pedestal had a line contour nearly identical with the normal Doppler line (Ref. 1). In practice this "Dicke (or collision) narrowing" is typically achieved by employing an inert buffer gas to reduce an atom or molecule's mean free path to less than the radiation wavelength. Under these conditions, however, the walls of Dicke's potential well move, and there is a high probability for forward scattering. As a consequence, though narrowed lineshapes are obtained, broad pedestals are neither predicted nor observed when buffer gas collisions dominate the narrowing process (Ref. 3).

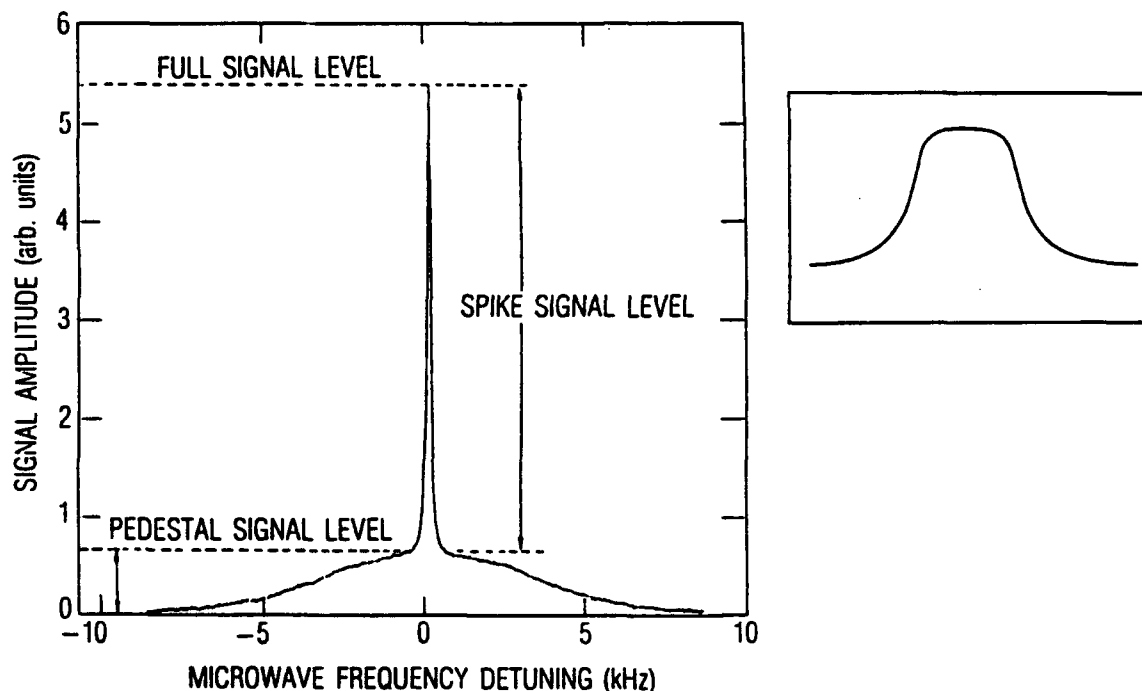


Figure 1. Typical Dicke-narrowed lineshape as obtained in our experiment: a narrow central-resonance spike sitting on top of a broad pedestal. Various signal levels are indicated. Rabi frequencies were determined by measuring the spike width in the regime of power broadening, and using these values to calibrate our microwave attenuator settings. Inset figure shows the distorted lineshapes that were observed when the pedestal amplitude saturated; the spike in this inset is of negligible amplitude.

Recently there has been renewed interest in the process of collision narrowing as originally envisioned by Dicke, partly because it corresponds to the manner in which sub-Doppler resonances are obtained in certain atomic clocks and masers (Refs. 4,5). In these devices the atomic storage vessel forms the static potential well, and the vessel's inner walls are coated with a nonperturbing material so that velocity-changing collisions do not disturb the internal state of the atom. Unfortunately, though broad pedestals have been experimentally observed and theoretically predicted under these conditions, striking ambiguities have arisen with regard to the pedestal's width.

In storage vessels (i.e., resonance cells) coated with long chain alkanes (paraffins), Robinson and Johnson (Ref. 5) found a Gaussian pedestal with a width of about 9 kHz for the  $\text{Rb}^{87}$  0-0 hyperfine transition in a 200-cm<sup>3</sup> resonance cell. The normal Doppler linewidth under their experimental conditions (approximately room temperature) was 9.1 kHz. Robinson and Johnson's observation is consistent with Dicke's original calculations, and supports the notion that these pedestals are a remnant of Doppler broadening. Additionally, Camparo and Frueholz have observed pedestal widths (FWHM) of 9.2 kHz for this transition in room-temperature, paraffin-coated cells attached to a vacuum system.<sup>1</sup> However, in both classical (Ref. 6) and quantum mechanical (Ref. 7) three-dimensional Monte Carlo calculations of the Dicke-narrowing process,  $\text{Rb}^{87}$  0-0 hyperfine transition pedestal widths substantially narrower than the Doppler width have been predicted (i.e., pedestal widths on the order of 5 kHz). Furthermore, these predictions have been verified in Dicke-narrowing experiments that used atomic resonance cells coated with siloxane materials (Ref. 7).

To reconcile these differing experimental results, Frueholz and Camparo (Ref. 7) have argued that when approximately Doppler-width pedestals are observed, the ensemble of oscillators has a non-thermal speed distribution. Since polarized atoms yield the observed signal in the above experiments, the authors suggest that high-speed atoms scatter off the paraffin surface through a direct-inelastic channel, which preserves the atomic polarization of these fast atoms as a result of small atom-surface interaction times. Slower atoms trap on the paraffin surface, are depolarized to a greater degree, and consequently contribute less to the observed resonance. The authors then argue that in the siloxane coated cells all atoms scatter off the surface through a trapping-desorption channel, so that the speed distribution of the oscillators contributing to the observed (albeit lower) signal is thermal. Though this hypothesis<sup>2</sup> concerning the role of surface scattering channels reconciles the various observations and calculations of Dicke pedestal widths, a major question regarding the nature of the pedestal nonetheless remains: if the Dicke pedestal is an inhomogeneous remnant of the Doppler broadening, why should thermal speed distributions yield pedestal widths less than the Doppler width?

To address this question we undertook an experimental study of Dicke-narrowed lineshapes in the presence of strong resonant fields. As will be shown, our results are in striking disagreement with expectations based on the hypothesis that the pedestal is an inhomogeneous remnant of Doppler broadening. Rather, the evidence that we have obtained suggests that the pedestal is best understood in terms of the oscillator's response to the electromagnetic field's power spectral density as observed in its rest frame (Ref. 8). This conclusion suggests that the problem of collision-narrowing can be separated into two distinct parts: (a) As a result of the oscillator's motion, the stochas-

<sup>1</sup>J. C. Camparo and R. P. Frueholtz, unpublished.

<sup>2</sup>Experiments are now in progress at The Aerospace Corporation and Duke University to test the validity of this hypothesis.

tically varying Doppler shifts (i.e., discrete frequency jumps) give rise to a nonmonochromatic electromagnetic-field power spectral density in the oscillator's rest frame. In the process originally envisioned by Dicke, this spectral density is composed of a delta function spike resting on a broad pedestal, whose width is determined by the ensemble speed distribution. (b) The shape of the resonance must then be determined by the behavior of the oscillator in the presence of this nonmonochromatic field. This view of collision narrowing has strong ties to the behavior of quantum systems in the presence of stochastic fields (Ref. 9), and suggests that an understanding of one will have consequences for an understanding of the other.

## II. EXPERIMENT

The double resonance experiment employed in our study of Dicke-narrowed lineshapes has been described previously (Ref. 7). Briefly, as illustrated in Figure 2, light from a single-mode diode laser is tuned to the  $5^2P_{3/2}$  ( $F = 3, 2, 1$ ) -  $5^2S_{1/2}$  ( $F = 2$ ) optical transition of  $\text{Rb}^{87}$  at 780.2 nm, and creates a population imbalance between the alkali atom's two ground-state hyperfine levels (i.e.,  $F = 1$  and  $F = 2$ ) (Ref. 10). The Rb vapor is contained within a spherical Pyrex cell coated with a long chain alkane (tetracontane). The cell has a diameter of  $\sim 4$  cm, which is greater than one-half the transition wavelength, and ensures that the pedestal portion of the Dicke-narrowed lineshape will have a reasonably large amplitude compared to the spike portion of the lineshape. As a result of the optical pumping process, atoms are removed from the absorbing hyperfine manifold, and the light intensity transmitted by the Rb vapor (which is proportional to the number density of atoms in the absorbing state) is maximized. To observe the Dicke-narrowed hyperfine transition lineshape, the frequency of a microwave field emanating from a horn is slowly swept over the ground state ( $F = 2, m_F = 0$ ) - ( $F = 1, m_F = 0$ ) transition at 6835 MHz, and the light intensity transmitted by the vapor is monitored.

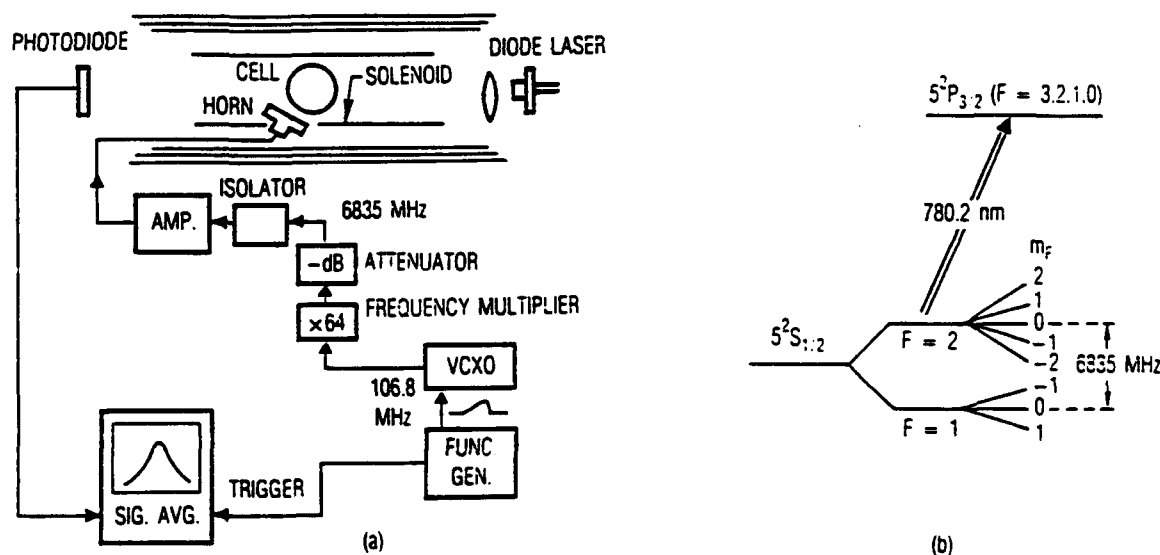


Figure 2. (a) Optical-pumping, double-resonance experimental arrangement for observing the  $\text{Rb}^{87}$  0-0 hyperfine transition lineshape. VCXO is voltage-controlled crystal oscillator. (b) Energy level diagram of  $\text{Rb}^{87}$  showing atomic transitions of interest.

Figure 1 is an example of two Dicke-narrowed lineshapes obtained in our experiment. In the limit of low optical-pumping rates and microwave Rabi frequency, we find that the linewidth of the spike is 70 Hz (linewidth will always imply full-width at half-maximum unless otherwise noted),

while the pedestal displays a linewidth of 7.3 kHz; the Doppler width of this transition under our experimental conditions (room temperature) is 9.1 kHz. Though this pedestal width is smaller than the Doppler width, in other experiments on paraffin-coated cells we have observed approximately 9-kHz pedestals. This cell was chosen for the present study, however, because it gave the best example of Dicke's standard spike and pedestal lineshape. The lineshape shown in the inset was observed under extreme saturation broadening conditions, and will be discussed subsequently.

To explain the sub-Doppler pedestal width, we believe that either the critical speed for trapping on this paraffin surface is low (i.e., the polarized atom speed distribution is relatively close to thermal) (Ref. 7), or there is a small trace of foreign gas in the cell due to outgassing over the cell's lifetime. Based on Monte Carlo calculations similar to those of Ref. 7, we estimate that any foreign gas in the resonance cell would have a pressure no greater than a few millitorr, and experiments performed at Duke University tend to substantiate this conclusion.<sup>3</sup> (All Monte Carlo calculations associated with the present work described the dynamic evolution of the quantum mechanical oscillator in terms of the density matrix.) At this foreign gas density, pressure broadening of the 0-0 hyperfine transition is expected to be less than  $\sim 10$  Hz (Ref. 11), which is negligible on the scale of the pedestal width. Further indication of insignificant foreign-gas pressure broadening comes from our observation of a 70-Hz spike linewidth, which includes contributions from the optical pumping rate and the wall relaxation rate (Ref. 12). Thus, though a small amount of foreign gas could affect the Dicke-narrowing process slightly, by altering speed distributions and atomic trajectories, it could not change an inhomogeneously broadened pedestal into a homogeneous one. Similarly, a different polarized atom speed distribution, due to an altered critical speed for trapping on the paraffin surface, would have no effect on the inhomogeneous or homogeneous character of the pedestal.

We examined the spike linewidth as a function of the microwave power attenuator settings, and found it to be a linearly increasing function of field strength. Since the spike signal shape is determined by the 0-0 hyperfine transition lineshape in the absence of Doppler broadening, its saturation behavior is well understood. Specifically, if care is taken to ensure that saturated hyperfine transition linewidths are not enhanced by relatively high optical pumping rates, then the 0-0 hyperfine transition linewidth is equal to twice the Rabi frequency (Ref. 13). Thus, the saturation broadening behavior of the spike could be used to calibrate the microwave power attenuator settings to Rabi frequency.

---

<sup>3</sup> In an experiment performed at Duke University, a cell that was sealed under high vacuum was opened several months later and its volatile contents examined. It was found that the cell contained approximately 1 millitorr of helium and 3 millitorr of hydrogen. Concerning the present cell, it was sealed under a pressure of  $10^{-7}$  torr approximately one month prior to the conclusion of these experiments.

### III. RESULTS AND ANALYSIS

#### A. Saturation Broadening

Figure 3 illustrates the saturation behavior of the Dicke-narrowed lineshape's amplitude. For nearly all field strength values employed in our experiment, the full signal level was at or near its saturated value. Note that as the field strength increased, the pedestal amplitude also increased (until it reached the signal saturation level). For the data of Figure 3, saturation of the pedestal amplitude occurred at a Rabi frequency of  $\sim 400$  Hz. Beyond this critical Rabi frequency, increases in field strength led to distortions in the shape of the pedestal (i.e., the pedestal appeared as if its top portion had been flattened). An example of this distorted shape is shown by the inset of Figure 1.

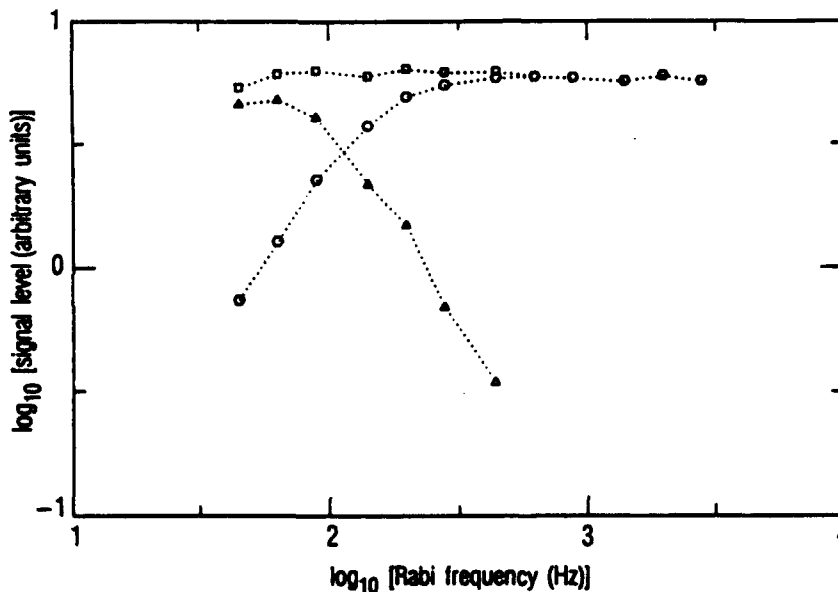


Figure 3. Saturation behavior of full signal amplitude ( $\square$ ), spike signal amplitude ( $\Delta$ ), and the pedestal amplitude ( $\circ$ ).

The distortions observed at these high Rabi frequencies are not easily explained by saturation broadening of an inhomogeneous resonance lineshape (Ref. 14), which in the case of Doppler broadening is expected to be a Voigt profile (i.e., the convolution of a Gaussian with a power broadened Lorentzian). For field strengths below the saturation value, an inhomogeneous lineshape will increase in amplitude, but typically will not change its general appearance. For field strengths above the saturation value, each individual Lorentzian undergoes saturation broadening, and in the limit of very high fields the observed lineshape takes on the form of a homogeneous Lorentzian. In general, however, the inhomogeneous lineshape does not change its shape as drastically as indicated by the inset of Figure 1. Thus, even if one were willing to accept that inhomogeneous

geneous widths less than the 9-kHz Doppler value were possible, it would be difficult to explain the anomalous shape of the saturated resonances.

Stronger evidence indicating that the Dicke pedestal is not a remnant of Doppler broadening is provided by the variation of the pedestal linewidth with Rabi frequency. These data are shown in Figure 4, along with the results from two sets of theoretical calculations. The first set of theoretical values was obtained from Monte Carlo calculations (x), and it is clear that in this case theory (x) and experiment (O) agree fairly well. We attribute the slight discrepancy between theory and experiment to the fact that the Monte Carlo calculations consider an idealized two-level quantum system, whereas the  $\text{Rb}^{87}$  atom has a total ground-state degeneracy of eight (Ref. 13). In these Monte Carlo calculations, we chose a critical speed for trapping on the paraffin surface of  $1.4 \times 10^4$  cm/sec (Ref. 7), employed a dephasing rate of 35 Hz [40-Hz optical absorption rate and 15-Hz collisional relaxation rate (Ref. 13)],<sup>4</sup> and set the cell diameter equal to 4 cm.

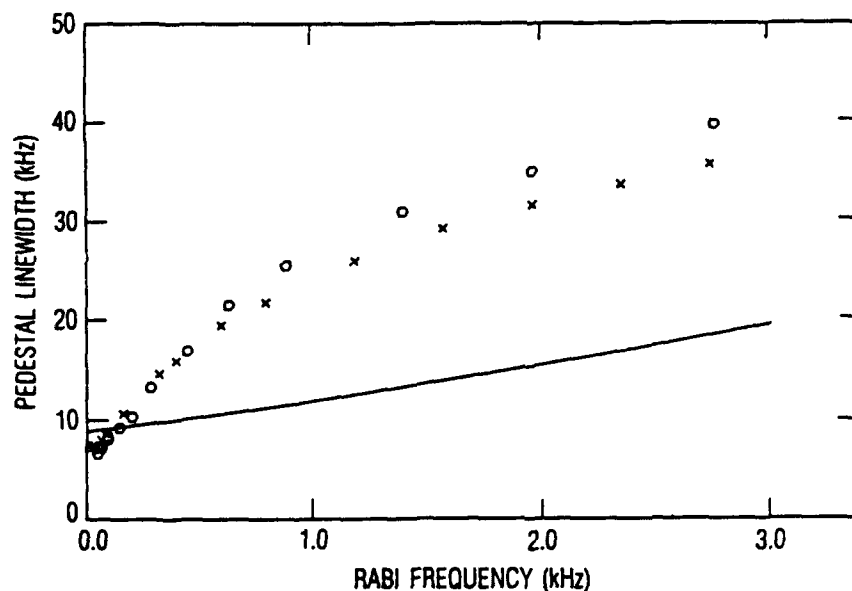


Figure 4. Power broadening behavior of the pedestal. Experimental data (O), and results from Monte Carlo calculations (x). The solid line presents theoretical linewidth values for an inhomogeneous Doppler-broadened Gaussian convolved with a power-broadened Lorentzian.

In addition to obtaining linewidth data from the Monte Carlo calculations, we have employed the calculations to investigate specific characteristics of the Dicke-narrowed lineshape. In the limit of very low Rabi frequencies, the Dicke-narrowed resonance can be described by a convolution of the atomic lineshape and the power spectral density of the radiation field as observed in the

<sup>4</sup> Since the optical pumping radiation only interacts with one of the states coupled by the microwave field, the dephasing rate due to optical pumping is one-half the optical photon absorption rate. See Ref. 13 for further details.

atom's rest frame. The form of this power spectral density is associated with the various Doppler shifts due to velocity changing collisions, and our calculations indicate that, in the rest frame of the atom, the field appears as a delta function spike sitting on top of a broad ( $\sim 7.3$  kHz) pedestal. (The power spectral density is generated by the Fourier transform of the time-varying Doppler shifts, which are obtained from the Monte Carlo atomic trajectories.) Furthermore, the calculations indicate that, in this particular cell geometry, only  $\sim 15\%$  of the field energy appears in the spike portion of the power spectral density. Since it is the spike portion of the power spectral density that gives rise to the spike portion of the observed signal, this observation suggests that Rabi frequencies determined by saturated spike linewidths underestimate the full-field Rabi frequency<sup>5</sup> by a factor of 2.6. This supposition is confirmed by the Monte Carlo lineshapes, which show that the power-broadened spike linewidth yields an "effective" Rabi frequency a factor of 2.6 smaller than the actual Rabi frequency employed in the calculations. (In the following portions of this report, all quoted theoretical Rabi frequencies will correspond to spike linewidth measurement values to facilitate comparison with experiment.) Finally, when we fit this power spectral density to a "generalized" Lorentzian shape (i.e.,  $\kappa/[A^2 + (\nu - \nu_f)^2]^n$ , where  $\nu_f$  is the field's central frequency) we find that the wings fall off approximately like  $\nu^{-5}$ .

The second set of theoretical values is shown in Figure 4 by the solid line curve, which corresponds to a theoretical calculation of Voigt profile saturation broadening (Ref. 15). In the Voigt profile calculations, we employed a 9.1-kHz Gaussian pedestal, composed of 70-Hz homogeneous Lorentzians that power broaden as the Rabi frequency is increased. Note that, at the highest Rabi frequencies investigated (3 kHz), the linewidth of the saturated Lorentzians would be  $\sim 6$  kHz, approximately equal to the width of the power spectral density's pedestal, but that the observed width of the Dicke lineshape pedestal is nearly an order of magnitude larger. Comparing the experimental data with the saturated Voigt profile calculations, it is clear that over the entire range of Rabi frequencies the agreement is quite poor. As a result of these investigations, we are forced to the conclusion that the assumption of an inhomogeneous Doppler broadened pedestal is untenable.

## B. Empirical Model of the Atom-as-Antenna

Since the pedestal cannot be interpreted as the remnant of a normal Doppler-broadened lineshape, we now have the task of rationalizing the pedestal's origin. In this endeavor it seems natural to associate the appearance of the Dicke pedestal with an interaction between the atom and the power spectral density's broad feature, and in this regard the saturation behavior of the pedestal appears to have strong ties to the interaction of quantum systems with stochastic fields (Ref. 9). As an initial attempt at rationalizing the origin of the pedestal, we view the atomic oscillator as a narrow-band antenna, which absorbs some fraction of the radiation field's total energy, depending upon the overlap of the radiation field and the atomic antenna's "response function." Consequently, in this "atom-as-antenna" analogy, the Rabi frequency that governs the quantum system's dynamic behavior is determined by that fraction of the field's energy that is "absorbed." At present we have no rigorous theoretical justification for this analogy; yet, as will be shown, we

<sup>5</sup> From the Monte Carlo calculations we have  $E_{\text{spike}}^2/E_{\text{total}}^2 = 0.15$ , where  $E$  is the field strength in the specified portion of the spectral density. Since the Rabi frequency  $\Omega$  is proportional to  $E$ ,  $\Omega_{\text{total}} = 2.6 \Omega_{\text{spike}}$ .

have achieved excellent and somewhat surprising agreement between this empirical theory and our experimental results.

To make the atom-as-antenna analogy quantitative, we focus our attention on the broad feature of the field's power spectral density. In the atom's rest frame, the power spectral density is well described by a generalized Lorentzian:

$$P(\nu)d\nu = \frac{|E_0|^2 \beta_n A^{2n-1} d\nu}{8\pi^2[(\nu - \nu_f)^2 + A^2]^n} \quad (1a)$$

where

$$\beta_n \equiv \sqrt{\pi} \frac{\Gamma(n)}{\Gamma(n-1/2)} \quad (1b)$$

Here,  $P(\nu)d\nu$  is the field energy density in the frequency range  $\nu$  to  $\nu + d\nu$ ;  $|E_0|^2/8\pi$  is the total field energy density;  $\nu_f$  is the frequency of the monochromatic field as observed in the laboratory frame, and  $A$  is related to the full width  $\Gamma$  [not to be confused with the gamma function  $\Gamma(m)$ ] of the field's spectral density in the rest frame of the atom:  $A = \Gamma/(2\sqrt{2^{1/n} - 1})$ . This choice of functional form has the merits that it: (a) is relatively general, (b) is symmetrical about  $\nu = \nu_f$ , and (c) reduces to the well-understood Lorentzian shape in suitable limits. The generalized Lorentzian was fit to the spectral density generated by our Monte Carlo calculations, and we found that  $n = 2.6$ .

We now invoke our antenna analogy and say that the appropriate Rabi frequency  $\omega_1$  for describing the dynamics of the field-atom interaction is determined by an overlap of the atomic antenna's (unit amplitude) response function  $L(\nu - \nu_a)$  and the field's spectral density:

$$\omega_1^2(\nu_a - \nu_f) = \int_0^\infty P(\nu - \nu_f) L(\nu - \nu_a) d\nu \quad (2)$$

Note that in this analogy the Rabi frequency depends on the detuning between the field and the atom ( $\nu_a - \nu_f$ ). We assume that the atomic antenna's response function is well approximated by the atomic absorption cross section within a frequency range on the order of the full-field Rabi frequency, and that beyond this range it drops to zero.<sup>6</sup>

$$L(\nu - \nu_a) = \gamma^2/[\gamma^2 + (\nu - \nu_a)^2] \quad (3)$$

Additionally, we restrict our attention to the case where the radiation field's power spectral density does not vary much over the atomic antenna response function (i.e.,  $\Gamma \gg \gamma$ ). With these assumptions, we find that

$$\omega_1^2(\delta) = \beta_n \gamma A^{2n-1} \Omega^2 / (\delta^2 + A^2)^n \quad (4)$$

<sup>6</sup> With regard to phase fluctuations, it is reasonable to assume that for  $|\nu - \nu_a|$  greater than the full-field Rabi frequency, the atoms would not absorb any radiant energy. This is a result of adiabaticity requirements for the dynamic response of the atom to rapid phase changes, as discussed in Ref. 16.

where  $\Omega$  is the Rabi frequency associated with the pedestal portion of the field's spectral density, and  $\delta \equiv \nu_a - \nu_f$ .

This Rabi's frequency is then substituted into the Bloch equations, which are solved in steady state. Note, though, that as far as the Bloch equations are concerned, the atom and electromagnetic field are in resonance; in the atom-as-antenna analogy, the field-atom detuning only enters the Bloch equations through its determination of the Rabi frequency  $\omega_1(\delta)$ . In this way one predicts that the observed signal  $S$  will have the form

$$S = [1 + \gamma(\delta^2 + A^2)^n / \beta_n A^{2n-1} \Omega^2]^{-1} \quad (5)$$

from which it is easy to show that the observed pedestal linewidth  $\Delta_{\text{ped}}$  will be

$$\Delta_{\text{ped}} = 2A \sqrt{(2 + \beta_n \Omega^2 / A^n)^{1/n} - 1} \quad (6)$$

Figure 5 shows the shape of these theoretical Dicke pedestals for two different values of the Rabi frequency. In Figure 5(a) the Rabi frequency is 100 Hz, which is just above the saturation value ( $\sim 35$  Hz), and the resonance clearly displays what would be considered a "normal" shape. Figure 5(b) shows the same resonance for a Rabi frequency of 3 kHz, approximately equal to the highest Rabi frequencies used in the present experiment, and, as was observed experimentally, the lineshape displays a flattened top. Consequently, with regard to its ability to predict qualitatively the anomalous saturated Dicke pedestal shapes, the empirical atom-as-antenna analogy does quite well.

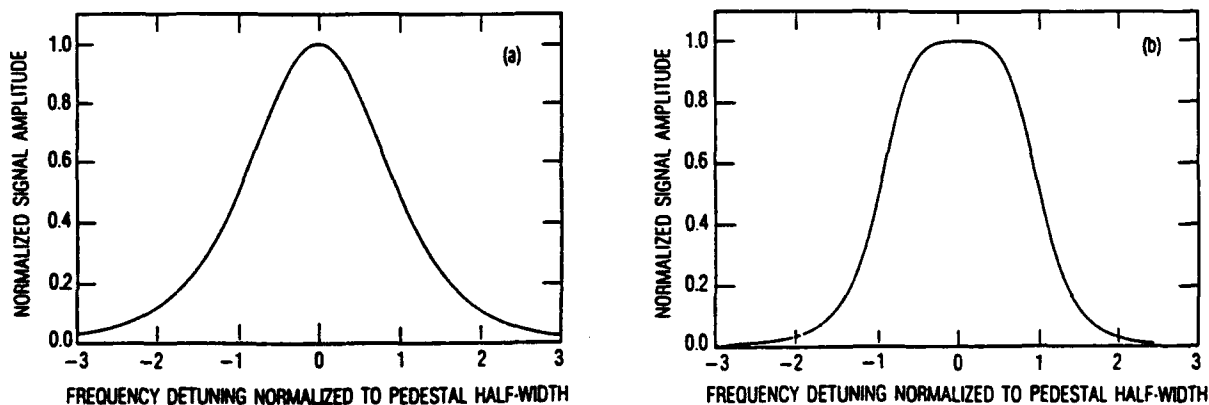


Figure 5. Predicted lineshapes in the atom-as-antenna analogy. (a) Relatively low Rabi frequency (100 Hz): the Rabi frequency is large enough to saturate the resonance, but not so large as to seriously distort the lineshape. (b) Relatively high Rabi frequency (3 kHz); here the lineshape is grossly distorted, displaying the flat-top appearance that was observed experimentally. In both calculations,  $n = 2.62$  and  $A = 6.663$  kHz.

The pedestal linewidth predicted by our empirical theory is shown in Figure 6, where the Monte Carlo (two-level quantum system) pedestal data have been reproduced for comparative purposes. Here, the solid curve corresponds to the pedestal linewidth predicted by Eq. (6) and our analytical spectral density formula, while the dashed line shows the results from numerical calculations using the actual Monte Carlo generated power spectral density in the atom-as-antenna analogy. Given the simplicity of this atomic antenna view of the atom in strong stochastic fields, it is remarkable that the empirical theory does so well in predicting the pedestal linewidths. The excellent agreement supports our previous contention that the Dicke pedestal is intimately associated with the interaction between the atom and the electromagnetic field's power spectral density as observed in the atom's rest frame. More importantly, however, is the fact that the excellent agreement indicates that the paradigm of the atom-as-antenna may have more general merit for describing the interaction of quantum systems with stochastic fields. Given the importance of understanding this latter question, it is desirable to test all possible anomalous predictions that this empirical theory makes.

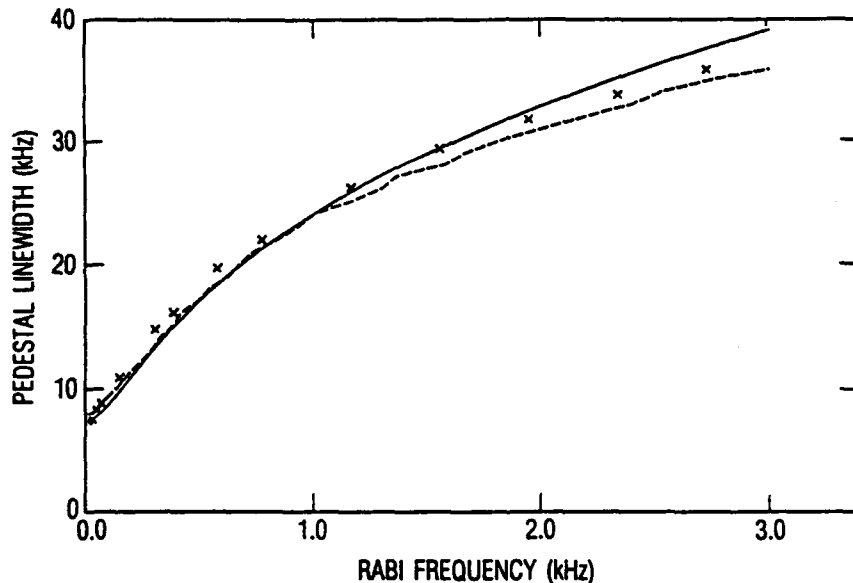


Figure 6. Saturation broadening of the pedestal linewidth in the atom-as-antenna analogy. Results from Monte Carlo calculations (x). The solid line is the prediction of pedestal linewidth based on Eq. (6) and our assumption of a generalized Lorentzian shape for the field's power spectral density. The dashed line is the result from a numerical atom-as-antenna calculation using the more accurate Monte Carlo generated spectral density.

### C. Light Narrowing of Dicke Pedestals

Examining Eq. (6) one finds that, in the atom-as-antenna analogy, the pedestal width is predicted to narrow as the atomic dephasing rate  $\gamma$  increases:

$$\Delta_{\text{ped}} \sim (\Omega^2/\gamma A)^{1/2n} \quad (\Omega^2 > \gamma A) \quad (7)$$

Such behavior is quite atypical, and its observation would lend strong support to the foregoing empirical theory. To test this prediction experimentally, we exploited the fact that in an optical pumping experiment the dephasing rate is linearly related to the optical absorption rate (Ref. 12). Thus, by removing neutral density filters from the laser beam path, illustrated in Figure 2, we were able to experimentally increase the quantum system's dephasing rate. Unfortunately, because the optical pumping rate enhances the power broadened linewidths in multiquantum level systems (Ref. 13), this procedure makes it difficult to compare quantitatively the atom-as-antenna theory with experiment. Nonetheless, the prediction can be tested for its qualitative agreement with experiment.

Experimental data for the pedestal linewidth as a function of normalized optical absorption rate are presented in Figure 7, and data obtained at two different values of the Rabi frequency are shown. It is clear that the predicted narrowing is present, and fairly substantial. For the 170-Hz Rabi frequency, it can be recognized that the observed narrowing of the pedestal linewidth is  $\sim 30\%$  (using the data of Figure 4). Assuming a 40-Hz optical absorption rate at the lowest intensity levels and a 15-Hz collisional relaxation rate, Eq. (6) also predicts  $\sim 30\%$  narrowing.<sup>7</sup>

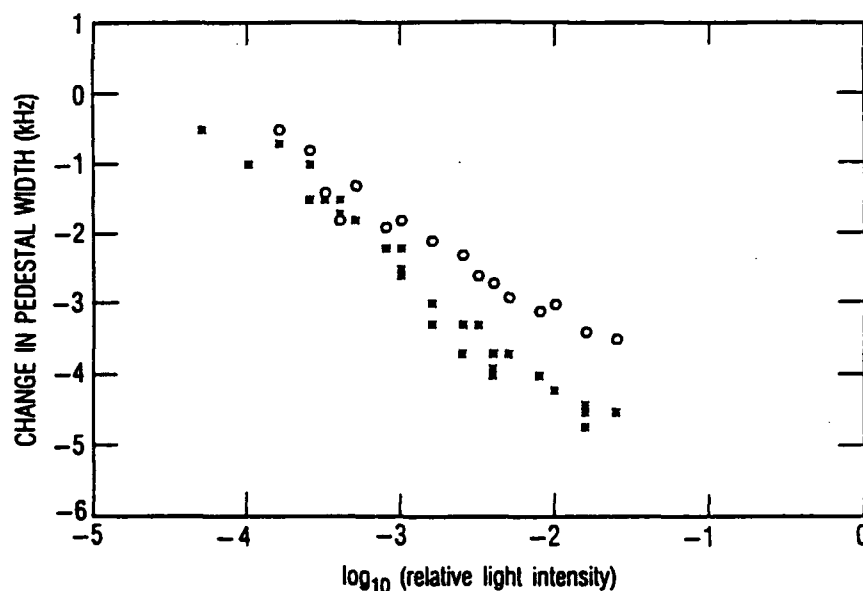


Figure 7. Observation of anomalous pedestal narrowing. (O) Rabi frequency of 170 Hz, as measured by the spike linewidth, and (\*) Rabi frequency of 870 Hz. In these experiments the quantum system's dephasing rate was increased by increasing the optical pumping rate. For the 170-Hz Rabi frequency (using the data presented in Figure 4) the narrowing effect is approximately 30% over the full light intensity range.

<sup>7</sup> Note that the Rabi frequency  $\Omega$  in Eq. (6) corresponds to the field strength in the pedestal portion of the spectral density. Hence, to compare with experiment we set  $\Omega$  equal to 92% of the total-field Rabi frequency. Thus, if the spike Rabi frequency is 170 Hz, we have  $\Omega = 408$  Hz; see Footnote 5.

#### IV. SUMMARY AND CONCLUSION

With regard to our initial motivation for the study of Dicke narrowing in strong fields, we have found that the long held assumption of an inhomogeneously broadened Doppler remnant pedestal is untenable. Further, the experimental data are inconsistent with inhomogeneously broadened pedestal lineshapes in general. Our results suggest, instead, that the pedestal is intimately connected with the electromagnetic field's power spectral density as observed in the rest frame of the quantum mechanical oscillator, which immediately suggests strong ties between the phenomena of Dicke narrowing and the important question of the behavior of quantum systems in stochastic fields. In this view of Dicke narrowing, the problem of understanding the narrowed lineshape divides naturally into two parts. First, there is the problem of understanding the electromagnetic field's power spectral density, which is related to the geometry of velocity-changing collisions, and ensemble speed distributions. Then, once this spectral density is known, there is the problem of understanding the behavior of the quantum system in the nonmonochromatic field.

Concerning this latter problem, we have found that viewing the quantum system as a narrow-band antenna has merit. In the atom-as-antenna analogy, one imagines that the quantum system only absorbs a fraction of the radiation field's energy. This fraction then determines the dynamic response of the system to the radiation field by means of the Bloch (density matrix) equations. Using this atom-as-antenna analogy, we have obtained very good agreement with experiment and our Monte Carlo calculations: (a) the analogy has predicted the anomalous shape of saturated pedestals; (b) it has yielded excellent agreement with Monte Carlo calculations of the saturated pedestal width; and (c) the analogy has predicted the experimentally verified relaxation narrowing of the pedestal. We believe that this same analogy may have broader implications for understanding the behavior of quantum systems in stochastic fields.

In this regard it is worth considering Eqs. (5) and (6) for  $n = 1$  (i.e., a Lorentzian spectral density). We then find that the observed resonance has a Lorentzian shape, with a linewidth given by

$$\Delta_{\text{ped}} = 2\sqrt{A^2 + (A/\gamma)\Omega^2} \quad (8)$$

This expression is similar to what would be obtained for a two-level quantum system in the presence of a monochromatic field, except the quantum system's dephasing rate  $1/T_2$  has been replaced by the field halfwidth  $A$ . For comparative purposes we note that Georges and Lambropoulos have rigorously analyzed the problem of two atomic levels coupled by a phase diffusing field (i.e., Lorentzian power spectral density) using a density matrix formalism (Ref. 17). They found that the single photon resonance is a Lorentzian with a linewidth  $\Delta_{\text{GL}}$ :

$$\Delta_{\text{GL}} = 2\sqrt{(A + \gamma)^2 + [(A + \gamma)/\gamma]\Omega^2} \quad (9)$$

This formula is very similar to Eq. (8), and in the limit that  $A \gg \gamma$  the two expressions are equivalent.<sup>8</sup> Therefore, not only does the atom-as-antenna analogy have merit in the analysis of Dicke-narrowed lineshapes, but given this result it appears that the analogy may have more general validity for describing the behavior of quantum systems in the presence of stochastic fields.

Though this analogy is intriguing, much remains to be done before its utility is truly established. First, given the agreement between this empirical theory and the Monte Carlo calculations, it should be possible to arrive at the atom-as-antenna analogy through the two-level density matrix equations. Such an analysis would indicate the approximations that are made when evoking the analogy and, consequently, the limits to which this analogy may be taken. Additionally, it would be worthwhile to experimentally investigate the behavior of quantum systems in the presence of various stochastic processes, in particular stochastic amplitude variations. Though the above experimental and theoretical work indicates the analogy's apparent validity for stochastic phase and frequency variations, whether the analogy can be made to work for stochastic amplitude fluctuations is an entirely different question. Only at the conclusion of such studies will it be possible to evaluate the significance of the atom-as-antenna analogy, either as a fortuitous model that works reasonably well for phase fluctuating fields, or as a generally valid approximation that provides insight into the behavior of quantum systems in the presence of arbitrary stochastic fields.

---

<sup>8</sup> We note that if we define  $\gamma_1$  and  $\gamma_2$  as the "bare" atom longitudinal and transverse relaxation rates, then the two expressions are only equivalent when  $\gamma_1 = \gamma_2 = \gamma$ .

## REFERENCES

1. R. H. Dicke, *Phys. Rev.* **89**, 472 (1953).
2. J. P. Wittke and R. H. Dicke, *Phys. Rev.* **103**, 620 (1956).
3. J. I. Gersten and H. M. Foley, *J. Opt. Soc. Am.* **58**, 933 (1968); D. G. McCartan and N. Lwin, *J. Phys. B.* **10**, L17 (1977); A. S. Pines, *J. Mol. Spectrosc.* **82**, 435 (1980), and references therein.
4. D. Kleppner, H. M. Goldenberg, and N. F. Ramsey, *Phys. Rev.* **126**, 603 (1962).
5. H. G. Robinson and C. E. Johnson, *Appl. Phys. Lett.* **40**, 771 (1982).
6. R. P. Frueholz and C. H. Volk, *J. Phys. B* **18**, 4055 (1985).
7. R. P. Frueholz and J. C. Camparo, *Phys. Rev. A* **35**, 3768 (1987).
8. H. G. Robinson, in *Proceedings of the Sixteenth Annual Precise Time and Time Interval (PTTI) Applications and Planning Meeting*, Greenbelt, Maryland, 1984 (unpublished).
9. S. N. Dixit, P. Zoller, and P. Lambropoulos, *Phys. Rev. A* **21**, 1289 (1980), and references therein.
10. J. C. Camparo, *Contemp. Phys.* **26**, 443 (1985).
11. F. Hartmann and F. Hartmann-Boutron, *Phys. Rev. A* **2**, 1885 (1970).
12. W. Happer, *Rev. Mod. Phys.* **44**, 169 (1972); J. Vanier, *Can. J. Phys.* **47**, 1461 (1969).
13. J. C. Camparo and R. P. Frueholz, *Phys. Rev. A* **31**, 1440 (1985); *Phys. Rev. A* **32**, 1888 (1985).
14. A. M. Portis, *Phys. Rev.* **91**, 1071 (1953); T. G. Castner, *Phys. Rev.* **115**, 1506 (1959).
15. P. Minguzzi and A. DiLieto, *J. Mol. Spectrosc.* **109**, 388 (1985).
16. Camparo and Frueholz, *Phys. Rev. A.* **38**, 6143 (1988).
17. A. T. Georges and P. Lambropoulos, *Phys. Rev. A* **18**, 587 (1978).

## TECHNOLOGY OPERATIONS

The Aerospace Corporation functions as an "architect-engineer" for national security programs, specializing in advanced military space systems. The Corporation's Technology Operations supports the effective and timely development and operation of national security systems through scientific research and the application of advanced technology. Vital to the success of the Corporation is the technical staff's wide-ranging expertise and its ability to stay abreast of new technological developments and program support issues associated with rapidly evolving space systems. Contributing capabilities are provided by these individual Technology Centers:

**Electronics Technology Center:** Microelectronics, solid-state device physics, VLSI reliability, compound semiconductors, radiation hardening, data storage technologies, infrared detector devices and testing; electro-optics, quantum electronics, solid-state lasers, optical propagation and communications; cw and pulsed chemical laser development, optical resonators, beam control, atmospheric propagation, and laser effects and countermeasures; atomic frequency standards, applied laser spectroscopy, laser chemistry, laser optoelectronics, phase conjugation and coherent imaging, solar cell physics, battery electrochemistry, battery testing and evaluation.

**Mechanics and Materials Technology Center:** Evaluation and characterization of new materials: metals, alloys, ceramics, polymers and their composites, and new forms of carbon; development and analysis of thin films and deposition techniques; nondestructive evaluation, component failure analysis and reliability; fracture mechanics and stress corrosion; development and evaluation of hardened components; analysis and evaluation of materials at cryogenic and elevated temperatures; launch vehicle and reentry fluid mechanics, heat transfer and flight dynamics; chemical and electric propulsion; spacecraft structural mechanics, spacecraft survivability and vulnerability assessment; contamination, thermal and structural control; high temperature thermomechanics, gas kinetics and radiation; lubrication and surface phenomena.

**Space and Environment Technology Center:** Magnetospheric, auroral and cosmic ray physics, wave-particle interactions, magnetospheric plasma waves; atmospheric and ionospheric physics, density and composition of the upper atmosphere, remote sensing using atmospheric radiation; solar physics, infrared astronomy, infrared signature analysis; effects of solar activity, magnetic storms and nuclear explosions on the earth's atmosphere, ionosphere and magnetosphere; effects of electromagnetic and particulate radiations on space systems; space instrumentation; propellant chemistry, chemical dynamics, environmental chemistry, trace detection; atmospheric chemical reactions, atmospheric optics, light scattering, state-specific chemical reactions and radiative signatures of missile plumes, and sensor out-of-field-of-view rejection.